The anharmonic vibration of Li in lithium amide

B. Paik,[1,a)] T. Hasegawa,[2] I. Ishii,[3] A. Michigoe,[2] T. Suzuki,[3] M. Udagawa,[2] N. Ogita,[2] T. Ichikawa,[1,b)] and Y. Kojima[1]
[1]*Institute for Advanced Materials Research (IAMR), Hiroshima University, Higashi-Hiroshima 739-8530, Japan*
[2]*Graduate School of Integrated Arts and Sciences, Hiroshima University, Higashi-Hiroshima 739-8521, Japan*
[3]*Department of Quantum Matter, ADSM, Hiroshima University, Higashi-Hiroshima 739-8530, Japan*

(Received 2 March 2012; accepted 23 March 2012; published online 12 April 2012)

A large amplitude rattling-type anharmonic vibration of Li is possible without guest-host type structure, as we report here for tetragonal $LiNH_2$ crystal. The low temperature (0.4–300 K) specific heat capacity and Raman spectroscopy support the phonon model of site-specific Li activities governed by the symmetry of the potential energy distribution around the Li atoms in $LiNH_2$, which yields the anharmonic Li3 vibration (optical) in one direction (either X or Y axis of the crystal), while the Li1 and Li2 atoms remain silent. Our finding may help to correlate ionic conductivity, thermal, and hydrogenation properties of $LiNH_2$. © *2012 American Institute of Physics*. [http://dx.doi.org/10.1063/1.3703586]

Li-N-H system has been given significant importance, separately, as a reversible hydrogen storage material[1–3] and in the Li-ion conductor for solid state electrolyte.[4,5] The focus in the hydrogen energy research has been so far on the hydrogen containing $(NH_x)^-$ anion, which is targeted to release the hydrogen at fuel cell operating temperature (typically <400 K) by partially replacing Li with suitable elements,[6,7] while on the other hand, in Li-based solid-state electrolyte research, the target is to improve the conductivity of Li-ion. These two apparently different aspects, viz., hydrogen sorption and Li conductivity, were brought closer recently by David *et al.*[8] in explaining the hydrogenation in $LiNH_2/Li_2NH$. According to them,[8] the heart of the mechanism behind the phase transition ($LiNH_2 \rightarrow Li_2NH$) is mediated by virtue of the Li^+ migration. It is interesting to note that although Li^+ ions in $LiNH_2$ and Li_2NH undergo similar octahedral $\rightarrow$ octahedral/tetrahedral site-hopping, there was not enough understanding from this study[8] to identify what causes different Li^+ mobilities in these compounds. A recent molecular dynamics (MD) calculation[9] distinguished different Li ion mobilities in Li compounds including Li_2NH and $LiNH_2$; though, their calculation leads to the conclusion that Li_2NH can show Li mobility only above 700 K while $LiNH_2$ cannot show any Li conductivity. On contrary, the experiments at room temperature show ionic conductivity for $LiNH_2$ and Li_2NH, where Li_2NH has ionic conductivity several orders of magnitude higher than that in $LiNH_2$.[10,11] In one of these reports,[11] a possible explanation was given for different ion conductivities in complex hydrides prepared from $LiNH_2$ and $LiBH_4$. According to them,[11] Li mobility depends on the fraction of Li ion population, which occupies some specific sites with spherical space surrounded by the hydrogen atoms. However, it was difficult to identify the factors that make those Li sites "special." Anisotropy in ionic conductivity is another aspect, which is also difficult to visualize from this *ad-hoc* concept. Clearly, a phonon description (vibration) of the thermally activated disorder, which is widely accepted as the driving force behind the ionic conductivity, was missing in understanding the Li mobility in Li based compounds. In this letter, we make attempt to understand the reason behind different Li mobilities in Li-N-H system by studying the intrinsic phonon/heat propagation in single crystal Li compound considering $LiNH_2$ as a case study by taking the advantage of its stable, good quality single crystal, which is free from defects over a reasonable temperature range.

To address the basic understanding of the thermal properties in $LiNH_2$ as well as the specific issues mentioned above, we compare the experimentally observed specific heat capacity (C_p) data (measured on a single crystal $LiNH_2$ over a temperature range of 0.4 K to 300 K) with Raman spectroscopy data (obtained from a single crystal $LiNH_2$ from room temperature to 3.4 K) and combine these results with the *ab initio* calculation of $LiNH_2$. The single crystals of $LiNH_2$ were prepared by melting the powder $LiNH_2$ (95% purity, Aldrich) close to 630 K under 0.5 MPa NH_3 atmosphere. The x-ray diffraction confirmed the structure of the single crystal to be tetragonal with I-4 symmetry already reported.[12–14] This initial structure[12] was used for the *ab initio* calculation of phonon modes at the wavevector $\mathbf{q} = 0$ using ABINIT package[15,16] and the calculated result has been reported elsewhere.[17] To calculate phonon dispersion, we estimated inter-atomic force constants using Fourier interpolation method[18] on the $4 \times 4 \times 4$ q points mesh in the reciprocal space of the simple tetragonal cell. Phonon density of states (DOSs) was calculated by tetrahedron method. Specific heat capacity was calculated using this DOS.

An overall impression on the thermal properties of $LiNH_2$ is presented by comparing the calculated and the measured data of the temperature dependent C_p in Fig. 1. Calculated and measured C_p are reasonably close, especially at lower temperature range (<50 K). By fitting the

[a)]Current address: Materials Physics Application-Materials Chemistry (MPA-MC), Los Alamos National Laboratory, Los Alamos, New Mexico 87545, USA. Electronic mail: bpaik@lanl.gov.
[b)]Author to whom correspondence should be addressed. Electronic mail: tichi@hiroshima-u.ac.jp.

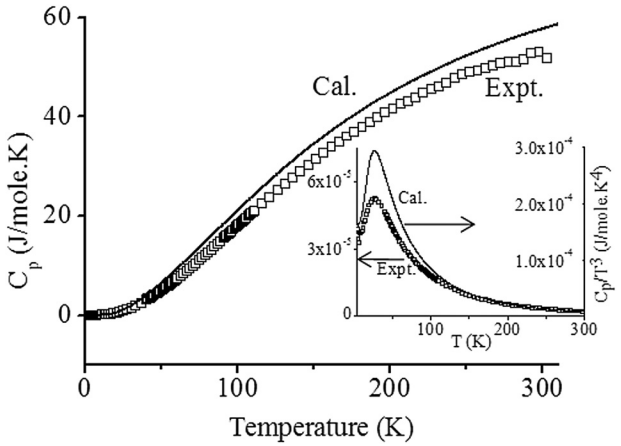

FIG. 1. Calculated (solid line) and measured (hollow square) specific heat capacity (C_p) of $LiNH_2$ within the temperature range 0.4–300 K. Inset: comparison between C_p/T^3 vs. T graphs using the calculated and measured C_p of $LiNH_2$. The peak in the C_p/T^3 vs. T graph is around 28 K for calculated and measured C_p.

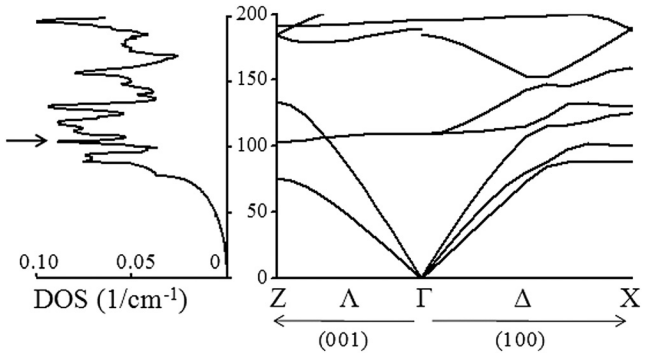

FIG. 2. Low frequency ($<200\,cm^{-1}$) phonon dispersion curve along with the associated DOS of $LiNH_2$ crystal (tetragonal). The peaks in the DOS are around $80\,cm^{-1}$, $90\,cm^{-1}$, $109\,cm^{-1}$, and $130\,cm^{-1}$. These vibrations constitute the peak at 28 K in C_p/T^3 vs. T graph in Fig. 1 (see text for further details). The arrow indicates $109\,cm^{-1}$ peak which contains Li3 optical mode of vibration.

experimental data, within this temperature range, into the equation $C_p = \gamma T + \beta T^3$, we have estimated $\gamma \rightarrow 0$ and $\beta = 0.038$ mJ mol^{-1} K^{-4}, where γ and β have their usual meaning. A very low γ value, estimated experimentally, suggests that the $LiNH_2$ crystal does not have significant electronic contribution in the C_p. This observation is the consequence of the non-metallic character of the $LiNH_2$ as reported by others.[19,20] From β, we experimentally estimate Debye temperature θ_D to be ~595 K. This value is comparable with the calculated θ_D 576 K for $LiNH_2$. In addition to estimating the basic thermal property and parameter, viz., C_p and θ_D, we also plot C_p/T^3 vs. T graph (inset of Fig. 1) to check for any special mode of vibration in $LiNH_2$ crystal. The peak around 28 K (corresponding phonon energy is 138 K or $96\,cm^{-1}$) in C_p/T^3 vs. T graph indicates possibility of some special mode of vibration including the independent oscillation (Einstein oscillation) as was routinely observed in the cage-type skutterudite or clathrate[21–23] structures, although $LiNH_2$ does not have any cage structure. That our first-principle calculation also predicts a peak in C_p/T^3 vs. T graph at around 28 K (Fig. 1, inset), we look into the details of the calculated low frequency phonon modes of $LiNH_2$ as an option to search for the origin of this peak.

Fig. 2 shows the phonon dispersion curve of low frequency modes ($<200\,cm^{-1}$) along with their DOS within the 1st Brillouin zone. By correlating the peak at 28 K (Fig. 1(b)) with the phonon modes in Fig. 2, the present *ab initio* calculation finds that this peak is contributed mainly by the optical mode of Li3 vibration ($109\,cm^{-1}$). We note that Li in the $LiNH_2$ lattice has three inequivalent positions, namely, Li1 at 2a site (0, 0, 0), Li2 at 2c site (0, 1/2, 1/4), and Li3 at 4f site (0, 1/2, z). Our calculation shows that, among all Li atoms, only Li3 is responsible for the optical mode at $109\,cm^{-1}$. The other contributors of the peak in Fig. 1 (inset) are the modes shown in Fig. 2 by the peaks around 80, 90, and $130\,cm^{-1}$. As a result, the peak in Cp/T^3 vs. T graph in Fig. 1 is broader than a typical sharp single-frequency Einstein oscillation. Solo contribution of Li3 in the optical mode is a clear indication that the vibrations of Li1 and Li2 are different from that of Li3 in $LiNH_2$. The discrete nature of Li vibrations gets further complicated as all Li3 atoms do not vibrate identically in $LiNH_2$. Classifying the Li3 atoms into two groups following the symmetry of the Li3 atom positions (Wyckoff notation 4f) in $LiNH_2$ crystal, viz., (1) $Li3_x$ with positions (0, 1/2, z) and (2) $Li3_y$ with positions (1/2, 0, −z), we find from our calculation that $Li3_x$ atoms vibrate along X-axis and the $Li3_y$ atoms vibrate along Y-axis. The first principles calculation also reveals that the nature of the vibration of the Li atoms, including the passive Li1, Li2, and the active Li3, is governed by the potential energy distribution around the Li atoms. The energy distribution surrounding Li1 and Li2 is narrow and deep in all directions yielding the curvatures of the potential surfaces that do not favor any atomic displacement, and therefore, Li1 and Li2 do not contribute in the phonon propagation. On the other hand, the potential well around Li3 sites is anisotropic. For $Li3_X$ atoms, the energy distribution favors atomic displacement in the X direction while the potential surface is deep and narrow along Y and Z directions. Symmetrically, the potentials are found to be deep and narrow along the X and Z directions, while allowing displacement along the Y direction for $Li3_Y$ atoms. Contrary to the Li1 and Li2 atoms, which always reside at the centre of the symmetric potential and cannot migrate to the interstitial positions, the Li3 atoms move far away instantly with rise in temperature. As a consequence, Li3 atoms are expected to undergo a large amplitude vibration. Anharmonic vibration of Li atom is a well-known phenomenon when Li is impurity (or guest) in a crystalline solid (host).[24–26] Our observation and model show that Li can demonstrate this localized vibration in crystalline solid, where Li is a part of the crystal, not a guest or impurity atom, as we show in $LiNH_2$ single crystal. We also note that the characteristic of the vibration we report here has similarity with that observed in the cage type structures[21–23] except that each Li3 vibration has single degree of freedom unlike the three degrees of freedom of each guest atom (Einstein oscillator) in the cage structure. Following these studies, where the rattling motion of guest atoms in the guest-host type structure has been claimed to be a universal phenomenon,[27] one can readily appreciate that the vibration frequency of Li3 atoms may increase with the temperature.[24–28] This property of large amplitude anharmonic vibration provides

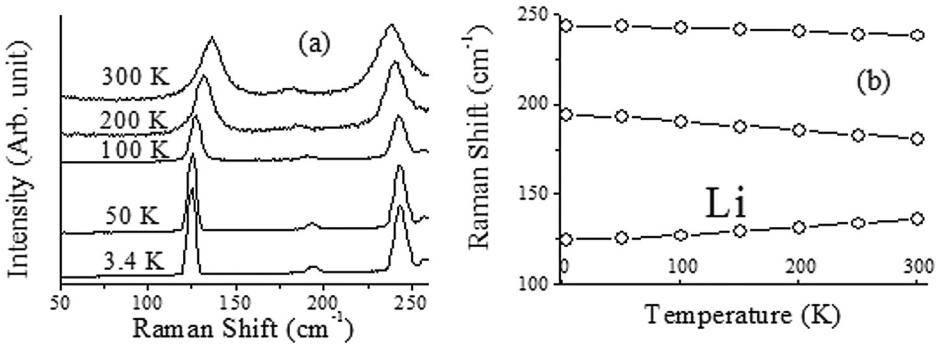

FIG. 3. (a) Low frequency (50–260 cm^{-1}) Raman spectrum of $LiNH_2$ single crystal within the temperature range 3.4–300 K. The vibration at 125 cm^{-1} has been identified as the optical Li3 vibration. (b) Effect of temperature on the Raman shift of the vibrations shown in (a). Energy of Li3 vibration increases with temperature (from 125 cm^{-1} at 3.4 K shifts to 137 cm^{-1} at 300 K).

an access tool to evident experimentally the vibration of Li3 atoms in $LiNH_2$ by exploring Raman spectroscopy, as discussed below.

A representative low-frequency (50–260 cm^{-1}) Raman spectrum of $LiNH_2$ single crystal within the temperature range 3.4–300 K is shown in Fig. 3(a) in which the peaks are identified according to the calculated Raman active modes.[17] The peak at 125 cm^{-1} in the low temperature (at 3.4 K) spectrum is identified as the Li3 vibration (E mode). It is to be noted here that our *ab initio* calculation predicts this energy to be 109 cm^{-1}, while the observed peak is at 125 cm^{-1}. In another report,[19] the calculated E mode in $LiNH_2$ is around 116–118 cm^{-1}, thus, showing discrepancy between the calculation and the experimental data. Nevertheless, identification of the Li3 vibration in the Raman spectroscopy is unambiguous as this peak should not be confused with any other Raman mode in $LiNH_2$, since there is no other peak in the vicinity of the lowest optical E mode. For example, the peak at 125 cm^{-1} in Fig. 3 (this peak appears at 109 cm^{-1} in the present calculation and at 116 cm^{-1} in the calculation by Miwa *et al.*[19]) has the nearest peak in the experimental spectrum at around 194 cm^{-1} (184 cm^{-1} in the present calculation and 192 cm^{-1} in Miwa *et al.*[19]), which is identified as a B mode. After identifying the Li3 vibration, it becomes straightforward to find out the evidence of Li3 rattling as we display the effect of temperature on the vibration energy of Li3 (Fig. 3(b)). One can appreciate from Fig. 3(b) that, with temperature, the Li vibration (E mode of 125 cm^{-1} at 3.4 K) shifts towards higher energy side (~137 cm^{-1} at 300 K), while the other Raman modes do not show any shift towards higher energy side. Thus, the Li3 phonon shows a typical finger print of anharmonic vibration, and therefore validates the model adopted in describing the rattling-type vibration of Li in $LiNH_2$ under the influence of the surrounding potential energy. As an overall consequence, the measured and the calculated specific heat capacity (C_p) and the Debye temperatures (θ_D) match closely (Fig. 1).

It is known by the contribution of a number of studies[3,14,29] that the phase transformation $Li_2NH \rightarrow LiNH_2$ is kinetically more favorable than the reverse one. The view of David *et al.*[8] supports this observation indirectly following the fact that the Li mobility, which is higher in Li_2NH than $LiNH_2$, triggers the hydrogenation mechanism. Two different perspectives of this aspect, viz., molecular dynamics describing the toggling of Li atoms among different interstitial positions and the thermodynamics of $Li_2NH/LiNH_2$ phase transformation (hydrogen sorption) may be brought closer by our study through the common platform of first principles calculation supported by the experiments as reported here. In addition, we also support the concept of site specific Li activities, which was introduced by Matsuo *et al.*[11]; though, in our report, we emphasize that the energy distribution around Li atoms (unlike the *ad-hoc* concept of volume of the spherical space around Li atom created by the hydrogen atoms[11]) is the key behind the site specific Li activities. We may also qualitatively explain the reason behind a finite (governed by the active Li sites) but weak (only 25% of total Li atoms are active either in X or Y direction) Li mobility in $LiNH_2$, which was not taken into account by MD calculation.[9]

Further implications of the findings in our study may also be important. Presence of site-specific Li activities may give scope of further application of Li-N-H system, in general, and for $LiNH_2$, in particular, which has a low thermal conductivity (not shown here). One of the factors causing the low thermal conductivity may be the interfering of rattling Li3 phonon with the heat carrying acoustic phonons, a property observed in *phonon glass*.[23] On the other hand, upon replacing Li1 and Li2 atoms by suitable elements (a similar approach is to weakening N-H bond for hydrogen desorption with partially substituting Li by K, Mg, and Ni in $LiNH_2$ (Refs. 6, 7 and 20), it may be possible to enhance the charge carriers in $LiNH_2$. Clearly, the proposed crystal may have interesting prospect as a thermoelectric material; similar to that of the phonon glass electron crystal (PGEC).[30] This future application is in addition to the on-going interest of $LiNH_2$ being one of the model Li-N-H systems as the hydrogen storage materials.

Authors acknowledge the financial contribution of NEDO HydroStar project of Government of Japan, the Grant-in-Aid (No. 20102005) for Scientific Research on Innovative Areas ("Heavy Electrons"), and the Grant-in-Aid (No. 20340093) from the Ministry of Education, Culture, Sports, Science and Technology of Japan. The calculated results in this paper have been obtained through the use of the ABINIT code, a common project of the Universite Catholique de Louvain, Corning Incorporated, and other contributors (URL http://www.abinit.org).

[1]P. Chen, Z. Xiong, J. Luo, J. Lin, and K. L. Tan, Nature (London) **420**, 302 (2002).
[2]P. Chen, Z. Xiong, J. Luo, J. Lin, and K. L. Tan, J. Phys. Chem. B **107**, 10967 (2003).
[3]H. Y. Leng, T. Ichikawa, S. Hino, N. Hanada, S. Isobe, and H. Fujii, J. Power Sources **156**, 166 (2006).

[4]M. Park, X. Zhang, M. Chung, G. B. Less, and A. M. Sastry, J. Power Sources **195**, 7904 (2010).
[5]A. Patil, V. Patil, D. W. Shin, J. Choi, D. Paik, and S. Yoon, Mater. Res. Bull. **43**, 1913 (2008).
[6]M. Gupta and R. P. Gupta, J. Alloys. Compd. **446–447**, 319 (2007).
[7]C. Zhang and A. Alavi, J. Phys. Chem. B **110**, 7139 (2006).
[8]W. I. F. David, M. O. Jones, D. H. Gregory, C. M. Jewell, S. R. Johnson, A. Walton, and P. P. Edwards, J. Am. Chem. Soc. **129**, 1594 (2007).
[9]A. Blomqvist, C. M. Araújo, R. H. Scheicher, P. Srepusharawoot, W. Li, P. Chen, and R. Ahuja, Phys. Rev. B **82**, 24304 (2010).
[10]B. A. Boukamp and R. A. Huggins, Phys. Lett. A **72**, 464 (1979).
[11]M. Matsuo, A. Remhof, P. Martelli, R. Caputo, M. Ernst, Y. Miura, T. Sato, H. Oguchi, H. Maekawa, H. Takamura, A. Borgschulte, A. Zuttel, and S.-I. Orimo, J. Am. Chem. Soc. **131**, 16389 (2009).
[12]M. H. Sørby, Y. Nakamura, H. W. Brinks, T. Ichikawa, S. Hino, H. Fujii, and B. C. Hauback, J. Alloys Compd. **428**, 297 (2007).
[13]J. B. Yang, X. D. Zhou, Q. Cai, W. J. James, and W. B. Yelon, Appl. Phys. Lett. **88**, 041914 (2006).
[14]T. Tsumuraya, T. Shishidou, and T. Oguchi, J. Alloys Compd. **446–447**, 323 (2007).
[15]X. Gonze, B. Amadon, P.-M. Anglade, J.-M. Beuken, F. Bottin, P. Boulanger, F. Bruneval, D. Caliste, R. Caracas, M. Côté *et al.*, Comput. Phys. Commun. **180**, 2582 (2009).
[16]X. Gonze, G.-M. Rignanese, M. Verstraete, J.-M. Beuken, Y. Pouillon, R. Caracas, F. Jollet, M. Torrent, G. Zerah, M. Mikami *et al.*, Z. Kristallogr. **220**, 558 (2005).
[17]A. Michigoe, T. Hasegawa, N. Ogita, M. Udagawa, M. Tsubota, T. Ichikawa, Y. Kojima, and S. Isobe, Chin. J. Phys. (Taipei) **49**, 294 (2011).
[18]X. Gonze and C. Lee, Phys. Rev. B **55**, 10355 (1997).
[19]K. Miwa, N. Ohba, S.-I. Towata, Y. Nakamori, and S.-I. Orimo, Phys. Rev. B **71**, 195109 (2005).
[20]J.-C. Crivello, M. Gupta, R. Cerný, M. Latroche, and D. Chandra, Phys. Rev. B **81**, 104113 (2010).
[21]V. Keppens, D. Mandrus, B. C. Sales, B. C. Chakoumakos, P. Dai, R. Coldea, M. B. Maple, D. A. Gajewski, E. J. Freeman, and S. Bennington, Nature (London) **395**, 876 (1998).
[22]Y. Takasu, T. Hasegawa, N. Ogita, M. Udagawa, M. A. Avila, K. Suekuni, and T. Takabatake, Phys. Rev. Lett. **100**, 165503 (2008).
[23]S. Paschen, W. Carrillo-Cabrera, A. Bentien, V. H. Tran, M. Baenitz, Yu. Grin, and F. Steglich, Phys. Rev. B **64**, 214404 (2001).
[24]T. Hattori, T. Nishii, and A. Mitsuishi, J. Phys. Soc. Jpn. **45**, 1287 (1978).
[25]D. Paul and S. Takeno, Phys. Rev. B **5**, 2328 (1972).
[26]W. Hayes, Phys. Rev. **138**, A1227 (1965).
[27]M. Udagawa, T. Hasegawa, Y. Takasu, N. Ogita, K. Suekuni, M. A. Avila, T. Takabatake, Y. Ishikawa, N. Takeda, Y. Nemoto *et al.*, J. Phys. Soc. Jpn. **77**(Suppl. A), 142 (2008).
[28]Y. Takasu, T. Hasegawa, N. Ogita, M. Udagawa, M. A. Avila, K. Suekuni, I. Ishii, T. Suzuki, and T. Takabatake, Phys. Rev. B **74**, 174303 (2006).
[29]S. Isobe, T. Ichikawa, K. Tokoyoda, N. Hanada, H. Y. Leng, Y. Kojima, and H. Fujii, Thermochim. Acta **468**, 35 (2008).
[30]G. S. Nolas, D. T. Morelli, and T. M. Tritt, Annu. Rev. Mater. Sci. **29**, 89 (1999).